A Closed-Form Approximation of Revisit Rate for Low-Altitude Spacecraft

Dr. Roger Chapman Burk, Ph.D.
Associate Professor, Department of Systems Engineering

Sponsored by
U.S. Army Space and Missile Defense Command, Future Warfare Center

Department of Systems Engineering
West Point, NY 10996
September 2011

DSE Technical Report: DSE-TR-1108
DTIC: ADA548618

Abstract

For many applications of low-altitude spacecraft, it is important to know how often the spacecraft revisits a given target. Average revisits per day can be calculated for a given scenario using astrodynamic software, but that approach can be tedious if a large number of cases are to be compared. This report develops a closed-form, continuous, and piecewise differentiable function that gives average revisits per day as a function of orbit altitude, orbit inclination, target latitude, and minimum required elevation. The function is compared to the results of astrodynamic simulations and shown to accurate to within 0.08 passes per day and 1% in almost all cases. It allows instant calculation of an excellent approximation of this important performance parameter, and could be used as part of an optimization routine. It will ease and speed architectural studies and provide more complete insight into how performance changes with orbit and target location. The convenience and flexibility provided by this function are demonstrated in a series of charts showing passes per day as a function of one, two, and three variables. The function assumes a circular orbit; the sensitivity of the result to eccentricity is explored using astrodynamic simulations, and is found to decrease by 5.3% as eccentricity increases to 0.07 for a typical case.

About the Author

Dr. Roger Chapman Burk has been on the faculty of the Department of Systems Engineering at the US Military Academy since 2000. He retired from the Air Force in 1995 after assignments in spacecraft mission control, spacecraft engineering, and mission analysis for the National Reconnaissance Office, and as director of the Graduate Space Operations program at the Air Force Institute of Technology (AFIT). He then worked in industry as a systems engineer and analyst for Science Applications International Corporation and The Aerospace Corporation before coming to USMA. He has an MS in Space Operations from AFIT and a PhD in Operations Research from the University of North Carolina at Chapel Hill. His research interests include decision analysis, space applications, and unmanned vehicles. He has published technical papers in *Military Operations Research*, *Interfaces*, and the journals of *Algorithms*, *Multi-Criteria Decision Analysis*, and *Guidance, Control, and Dynamics*. In 2007-08 he was a visiting associate professor at the Center for Innovation in Engineering Education at Princeton University.

Acknowledgements

This work was inspired by a cadet capstone project in 2009-10 done for the Future Warfare Center of the U.S. Army Space and Missile Defense Command. The problem was to recommend a constellation of spacecraft in low Earth orbits to track targets moving in a given terrestrial network. This required an estimation of the revisit rate for each candidate constellation. Instead of running astrodynamic software for case after case, the cadets used a geometric argument to approximate the long-term average revisit rate for each case. After the cadets graduated, I continued to think about their approach, how it could be generalized, and how accurate it really was. Eventually I was able to show that it was extremely accurate and could be generalized to cover all cases. These cadets, now all Army lieutenants, were Jordan E. Benson, Lesa B. Boyd, Alexander W. Farinelli, Brittany L. Fearnside, and Christopher M. Molaro. Then-cadet Benson did the bulk of the geometrical work.

Table of Contents

Abstract ..... **iii**

About the Author ..... **iv**

Acknowledgements ..... **v**

Table of Contents ..... **vi**

List of Figures ..... **viii**

List of Tables ..... **ix**

Chapter 1: Problem Description **10**

1.1 Problem Statement 10
1.2 Literature Survey 10
1.3 Problem Formulation 11
1.4 Assumptions and Limitations 12
1.5 Summary of Results 13
1.6 Organization 15

Chapter 2: Derivation **16**

2.1 Preliminary Calculations 16
2.2 Fraction of Revs that Include a Pass Assuming a Non-Rotating Earth (*f*) 16
2.3 Final Calculations 24

Chapter 3: Accuracy of the Approximation **25**

3.1 Cases Examined 25
3.2 Five Regions 25
3.3 Factorial Analysis 27
3.4 PPD as a Function of Latitude 27

Chapter 4: Excursions around a Base Case **30**

4.1 The Base Case 30

4.2 Varying One Parameter 30

4.3 Varying Two Parameters 33

4.4 Varying Three Parameters 38

Chapter 5: Sensitivity to Assumption of Circularity **40**

Chapter 6: Conclusion **43**

Bibliography **44**

Appendix A: List of Abbreviations **45**

Distribution List **46**

REPORT DOCUMENTATION PAGE – SF298 ..... **48**

List of Figures

Figure 1. Arguments of PPD(i,h,ε,L) 12
Figure 2. Minimum Required Earth Central Angle 16
Figure 3. Geometry for Revs with Passes 17
Figure 4. Angles φ_1 and φ_2 18
Figure 5. Geometry for Finding φ_2 19
Figure 6. Five Cases for f 21
Figure 7. Plot of Table 1 Data 26
Figure 8. Plot of Table 2 Data 28
Figure 9. Plot of Table 3 Data 29
Figure 10. PPD as a Function of i for the Base Case 31
Figure 11. PPD as a Function of h for the Base Case 31
Figure 12. PPD as a Function of ε for the Base Case 32
Figure 13. PPD as a Function of L for the Base Case 32
Figure 14. PPD as a Function of i and L, with h = 680 km and ε = 30° 33
Figure 15. PPD as a Function of ε and L, with h = 680 km and i = 60° 35
Figure 16. *PPD* as a Function of ε and i, with h = 680 km and L = 35° 35
Figure 17. *PPD* as a Function of h and i, with ε = 30° and L = 35° 37
Figure 18. *PPD* as a Function of h and L, with ε = 30° and i = 60° 37
Figure 19. *PPD* as a Function of h and ε, with L = 35° and i = 60° 38
Figure 20. *PPD* = 2.10 Surface (h = 680 km) 39
Figure 21. Variation of PPD with Eccentricity for Base Case 40
Figure 22. Month-to-Month Variation of PPD with Eccentricity for Base Case 41

List of Tables

Table 1. Calculation and STK Results in Figure 6 Regions 26

Table 2. 2^4 Factorial Analysis of Calculation vs. STK Results 28

Table 3. PPD as a Function of Latitude 29

Table 4. A Base Case 30

Table 5. Variation of PPD with Eccentricity for Base Case 40

Chapter 1: Problem Description

1.1 Problem Statement

One common measure of performance for low-altitude spacecraft is the revisit rate, often measured in average passes per day (PPD). Passes of spacecraft in low Earth orbit (LEO) are short; five minutes is typical. Each pass represents essentially one opportunity for a given spacecraft to visit a given terrestrial location for intelligence collection, surveillance, reconnaissance, or communication. With a large constellation of dozens of spacecraft one can achieve continuous coverage, but with small constellations it is more practical to speak of discrete visits to the target. The usual way to determine PPD for a given spacecraft-target pair is to run a simulation of the situation for several years using widely-available orbit propagation software such as STK (http://www.agi.com/products/by-product-type/applications/stk/) and divide the resulting number of passes by the number of days simulated. This is fairly easy and each simulation takes only seconds, but it still requires the analyst to select, set up, and run a discrete set of cases, and to take care that the cases are representative of the long-term behavior of the system. This report presents a closed-form approximation that will instantly and accurately calculate long-term average PPD as a continuous and piecewise differentiable function of spacecraft and target parameters. This will simplify and speed analysis of LEO architecture alternatives when PPD is an important measure of performance. With this formulation, PPD is a function that can be optimized.

1.2 Literature Survey

This report assumes a familiarity with basic orbital dynamics. Introductions to this topic can be found in Bate, Mueller, and White (1971) and Wertz (2001). The reader is also assumed to be familiar with basic spherical trigonometry.

Much work has been on LEO constellations for coverage of terrestrial targets, i.e. the total time or fraction of time that the target is in view from the satellite. The requirements for continuous coverage have received particular attention. Chapter 9 of Wertz (2001) provides analytical approximations for single-satellite coverage and Chapter 13 does the same for

constellation coverage. Additional recent work on coverage has been published by Santos and Shapiro (2007, 2008).

Revisit rate has received less attention. Lang (1984) worked on minimizing that maximum revisit time for a constellation. A fundamental contribution towards an analytical formula for PPD was made by Wertz (1999, 2001), who presented formulas that can be used to find approximate intervals around the Equator where an ascending node results in a pass over a given target. These formulas are central to the approximation developed in this report (eqns 13 and 14). However, Wertz did not provide a derivation, corrections for Earth's rotation or oblateness, or a unifying formula covering all cases. Sugrue (2007) developed Wertz's formulas by correcting the results for Earth's rotation and using them in algorithmic optimization, but she calculated PPD only for discrete cases rather than as a continuous function. This report builds on the contributions of Wertz and of Sugrue by providing a derivation for Wertz's formulas, by unifying them in a single formula that covers all cases, by including corrections for Earth's rotation and oblateness, by determining the resulting accuracy compared to the results of orbit propagation software, by determining sensitivity to the assumption of circular orbits, and by using the formula to illustrate how the PPD function varies when its arguments vary.

1.3 Problem Formulation

PPD will be expressed as a function of four variables: PPD(i,h,ε,L), with

$$\begin{aligned} i &\equiv \text{inclination of the spacecraft's orbit, } 0 \le i \le \pi \\ h &\equiv \text{altitude of the spacecraft's orbit, } 0 \le h \\ \varepsilon &\equiv \text{minimum elevation above the horizon required for a pass, } 0 \le \varepsilon \le \pi/2 \\ L &\equiv \text{north or south latitude of the target, } 0 \le L \le \pi/2 \end{aligned} \tag{1}$$

These parameters are illustrated in Figure 1.

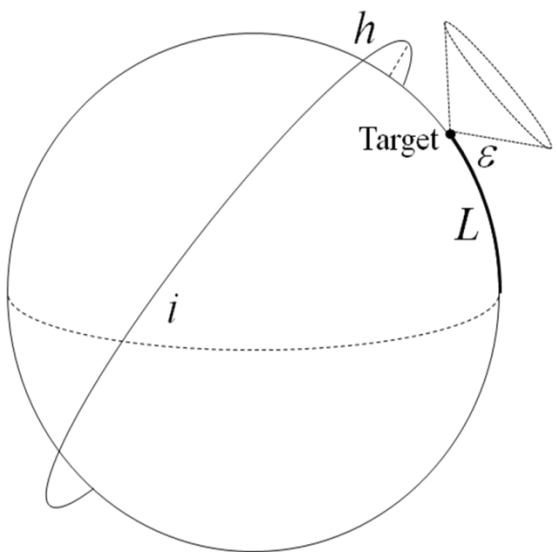

Figure 1. Arguments of PPD(*i*,*h*,*ε*,*L*)

1.4 Assumptions and Limitations

The PPD formula developed in this report gives a long-term average of passes per day. All passes count equally, whether they are short or long: a one-second pass counts equally with a ten-minute pass. (Passes too short to be useful can be excluded by increasing the minimum required elevation ε, at the cost of possibly missing some low-elevation but long-duration passes.) All passes count equally whether they are of low or high elevation, as long as the maximum elevation of the pass is greater than ε. All passes count regardless of local time of day. The passes may be distributed throughout the day or grouped together, though passes cannot be much closer together than one orbital period (about ninety minutes). In fact, the usual distribution is for there to be one or two sets of consecutive orbits (revolutions, revs) each day that include passes over a given target, each set followed by consecutive revs without passes. The formula gives no information on the duration of passes, percent coverage, or coverage gaps. It also gives no information on revisit time except for an upper limit on long-term average revisit time: 1/PPD.

The target is assumed to be at sea level. There is no accounting for obscura at the target's horizon and no correction for atmospheric refraction.

The spacecraft is assumed to be in a circular orbit that is not decaying (0 explores sensitivity to the assumption of zero eccentricity). The longitudes of ascending nodes are

assumed to be randomly and uniformly distributed around the Equator. If an orbit is maintained such that the orbital period evenly divides a sidereal day, then the spacecraft's ground tracks will repeat, this assumption will be violated, and the formula will not be accurate. Successive longitudes are not independent, being determined by orbital mechanics, but that is immaterial to this calculation of a long-term average.

Finally, the PPD approximation is intended for spacecraft in low Earth orbit, say those with an altitude of 6,000 km or less or a period of four hours or less. The formula remains valid for higher orbits, but as orbits get higher, the passes become very long (unless ε is very large) and it is more useful to speak of periods of coverage than of discrete passes. Of course, the formula will not work for geosynchronous spacecraft, whose "passes" last indefinitely.

1.5 Summary of Results

Though the formula for PPD(i,h,ε,L) is in closed form, it is not particularly simple. By heroic effort it could be put into a single equation or line of code, but for most purposes it is better to calculate it via a series of intermediate results. The required calculations are summarized here for convenience; they are derived and justified in the body of this report.

The arguments of the function are defined at (1) above. The constants used in the function are:

r_E	equatorial radius of the Earth (~6378.145 km)	
e_E	oblateness eccentricity of the Earth (~0.08182)	(2)
μ	gravitational parameter of the Earth (~398601 km^3/s^2)	
D	duration of a solar day (86400 s)	

The calculation proceeds as follows. First calculate the Earth central distance of the target (r_L):

$$r_L = r_E \sqrt{\frac{\cos^2 L + (1-e_E^2)^2 \sin^2 L}{1-e_E^2 \sin^2 L}} \tag{3}$$

Then find the maximum Earth central angle for a pass (λ):

$$\lambda = \frac{\pi}{2} - \varepsilon - \arcsin\left(\frac{r_L}{r_E + h}\sin\left(\frac{\pi}{2} + \varepsilon\right)\right) \tag{4}$$

Calculate the fraction of revs that include a pass over the target assuming a non-rotating Earth (f), via a set of intermediate results that are explained in the next chapter:

$$F_1 = \begin{cases} \operatorname{sign}\left(L-\lambda\right) & \text{if } i = 0 \\ \operatorname{sign}\left(\pi/2-\lambda-\min(i,\pi/2-i)\right) & \text{if } L = \pi/2 \\ \dfrac{-\sin\lambda+\sin L\cos i}{\cos L\sin i} & \text{otherwise} \end{cases} \tag{5}$$

$$\varphi_1 = \arccos\left\{\min\left[1,\max\left(-1,F_1\right)\right]\right\} \tag{6}$$

$$F_2 = \begin{cases} 1 & \text{if } i = 0 \text{ or } L = \pi/2 \\ \dfrac{\sin\lambda+\sin L\cos i}{\cos L\sin i} & \text{otherwise} \end{cases} \tag{7}$$

$$\varphi_2 = \arccos\left\{\min\left[1,F_2\right]\right\} \tag{8}$$

$$f = \frac{\varphi_1-\varphi_2}{\pi} \tag{9}$$

Find the orbital period (P):

$$P = 2\pi\sqrt{(r_E+h)^3/\mu} \tag{10}$$

And finally calculate passes per day:

$$\text{PPD} = \left(\frac{D}{P}-\cos i\right)f \tag{11}$$

This approximation is quite accurate when compared to the results of orbit propagation. In the set of cases examined, the largest errors occurred in the vicinity of $L \pm \lambda = i$ or $\pi - i$, when the error could be as great as 0.22 PPD. When more than two degrees from those inclinations, the error was never more than 0.08 PPD and never more than 1%.

1.6 Organization

The next chapter of this report justifies equations (3) through (11) above. Chapter 3: explores the accuracy of the approximation compared to the results of orbit propagation software. Chapter 4: uses the approximation to show how PPD varies as the formula's arguments are varied around a base case. 0 explores the sensitivity of the formula to the assumption that the spacecraft's orbit is circular. 0 gives some concluding remarks.

Chapter 2: Derivation

2.1 Preliminary Calculations

The formula for r_L (3), the Earth central distance of the target as a function of latitude, can be found easily from formulas for its geocentric coordinates given in Bate, Mueller, and White (1971, p. 98, eqn 2.8-7). This is a small correction, and for many purposes r_L could be approximated by r_E. However, the difference in PPD can be noticeable at high latitudes.

The formula for λ (4), the minimum Earth central angle between the target and the spacecraft for a pass, can be found from the trigonometry of the situation, which is shown in Figure 2. We have $\pi/2+\varepsilon + \theta + \lambda = \pi$, and an expression for sin θ comes from the law of sines.

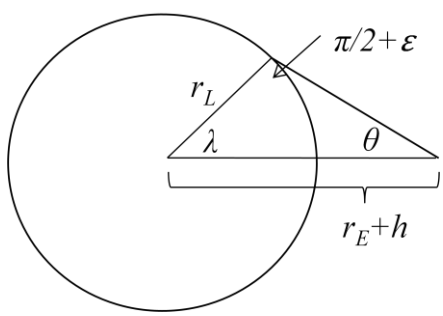

Figure 2. Minimum Required Earth Central Angle

2.2 Fraction of Revs that Include a Pass Assuming a Non-Rotating Earth (f)

The formula for f is the most involved part of the calculation. We start by considering a non-rotating spherical Earth and assuming that longitudes of ascending nodes are uniformly distributed around the Equator [the effect of Earth's rotation will be accounted for by the cos i term in (11)]. The revs with passes will be those whose ground track crosses a circle of angular radius λ centered at the target. For example, in Figure 3 the revs with passes will be those with ascending nodes in intervals FG and HA. By symmetry, FG=HA, so f = HA/π.

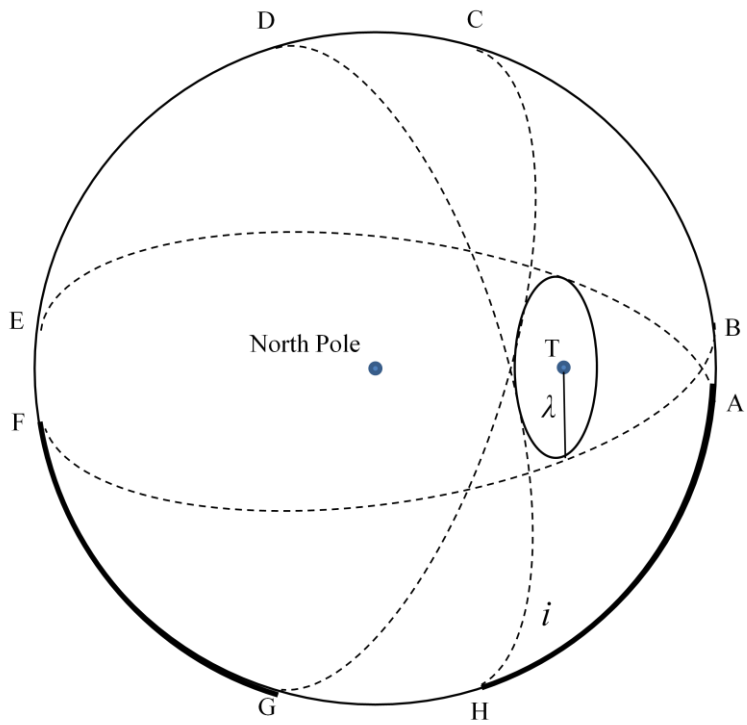

Figure 3. Geometry for Revs with Passes

(Looking down from celestial north. Circumference is the Equator. Target is at T.)

If we define the angles φ_1 and φ_2 along the Equator from the meridian 90 degrees west of the target to the ascending nodes A and H, as shown in Figure 4, then

$$f = \frac{HA}{\pi} = \frac{\varphi_1 - \varphi_2}{\pi} \tag{12}$$

We can find φ_1 by considering the two right spherical triangles TJI and KJA, which have vertical angles at J.

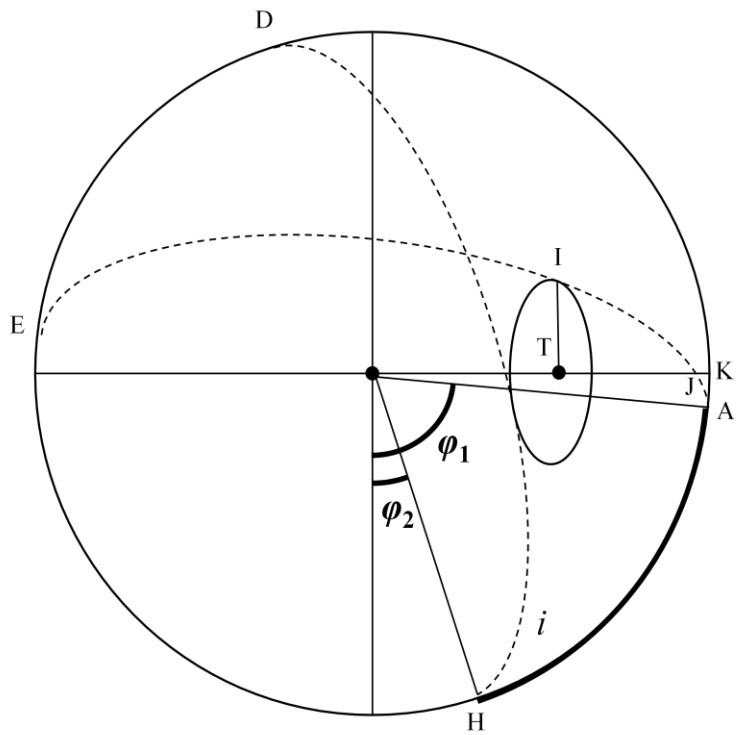

Figure 4. Angles φ_1 and φ_2

Applying Napier's rules to these two triangles, we can get an expression for the tangent of arc JK:

$$\sin \mathrm{TJI} = \sin \mathrm{KJA}$$

$$\frac{\cos \mathrm{JAK}}{\cos \mathrm{JK}} = \frac{\sin \mathrm{TI}}{\sin \mathrm{TJ}}$$

$$\frac{\cos i}{\cos \mathrm{JK}} = \frac{\sin \lambda}{\sin \mathrm{TJ}}$$

$$\sin \mathrm{TJ} = \frac{\sin \lambda \cos \mathrm{JK}}{\cos i}$$

$$\sin(\mathrm{TK} - \mathrm{JK}) = \sin(L - \mathrm{JK}) = \frac{\sin \lambda \cos \mathrm{JK}}{\cos i}$$

$$\sin L \cos \mathrm{JK} - \cos L \sin \mathrm{JK} = \frac{\sin \lambda \cos \mathrm{JK}}{\cos i}$$

$$\sin L - \cos L \tan \mathrm{JK} = \frac{\sin \lambda}{\cos i}$$

$$\tan \mathrm{JK} = \frac{\sin L - \sin \lambda / \cos i}{\cos L} = \tan L - \frac{\sin \lambda}{\cos i \cos L}$$

Now applying Napier's rules to triangle KJA:

$$\sin \mathrm{KA} = \frac{\tan \mathrm{JK}}{\tan \mathrm{JAK}}$$

$$\sin\left(\frac{\pi}{2} - \varphi_1\right) = \frac{\tan \mathrm{JK}}{\tan i} = \frac{\tan L - \dfrac{\sin \lambda}{\cos i \cos L}}{\tan i}$$

$$\cos \varphi_1 = \tan L \cot i - \frac{\sin \lambda \cot i}{\cos i \cos L}$$

$$\cos \varphi_1 = \frac{\sin L \cos i}{\cos L \sin i} - \frac{\sin \lambda}{\cos L \sin i}$$

$$\cos \varphi_1 = \frac{-\sin \lambda + \sin L \cos i}{\cos L \sin i} \tag{13}$$

Similarly, for φ_2 we can find another two spherical triangles sharing a vertical angle: LMP and NMT in Figure 5.

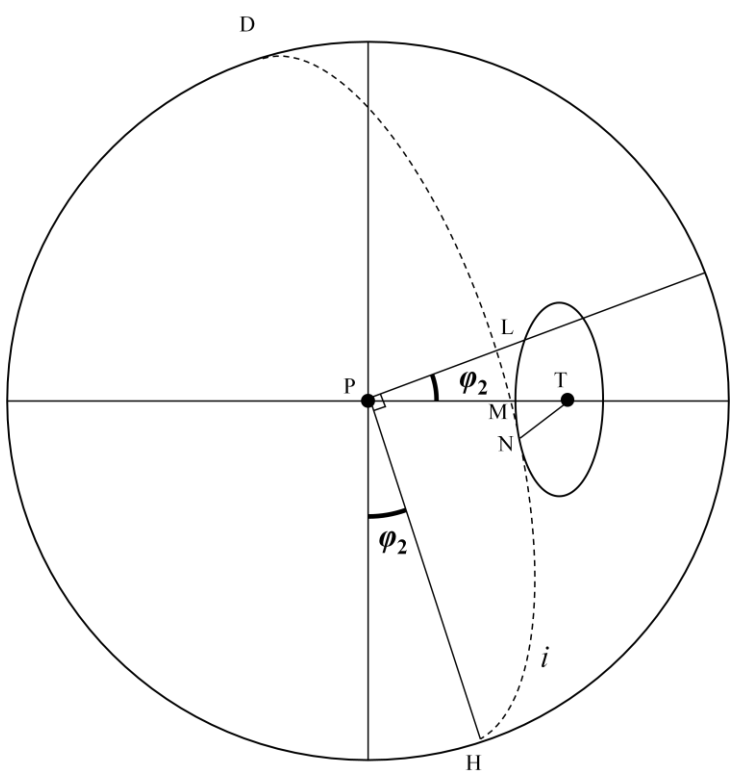

Figure 5. Geometry for Finding φ_2

$$\frac{\sin \mathrm{PL}}{\sin \mathrm{PM}} = \frac{\sin \mathrm{NT}}{\sin \mathrm{MT}}$$

$$\frac{\sin(\pi/2 - i)}{\sin \mathrm{PM}} = \frac{\sin \lambda}{\sin\left(\pi/2 - L - \mathrm{PM}\right)}$$

$$\cos i \cos(L + \mathrm{PM}) = \sin \lambda \sin \mathrm{PM}$$

$$\cos L \cos \mathrm{PM} - \sin L \sin \mathrm{PM} = \frac{\sin \lambda \sin \mathrm{PM}}{\cos i}$$

$$\cos L \cot \mathrm{PM} - \sin L = \frac{\sin \lambda}{\cos i}$$

$$\cot \mathrm{PM} = \frac{\sin \lambda / \cos i + \sin L}{\cos L} = \tan L + \frac{\sin \lambda}{\cos i \cos L}$$

$$\begin{aligned}
\cos \varphi_2 &= \frac{\tan \mathrm{PL}}{\tan \mathrm{PM}} = \frac{\tan(\pi/2 - i)}{\tan \mathrm{PM}} = \cot \mathrm{PM} \cot i \\
&= \left(\tan L + \frac{\sin \lambda}{\cos i \cos L}\right) \cot i \\
&= \frac{\sin L \cos i}{\cos L \sin i} + \frac{\sin \lambda}{\cos L \sin i} \\
&= \frac{\sin \lambda + \sin L \cos i}{\cos L \sin i} \qquad (14)
\end{aligned}$$

We have derived formulas that give us φ_1 and φ_2 for the geometry in Figure 4, in which the target is in the northern hemisphere and $\pi/2 \geq i \geq L+\lambda$, i.e. the inclination is high enough that the spacecraft can pass north of the target without seeing it, but is still prograde. Thus we have f for this geometry. The rest of this section shows that the formula for f works for all geometries if we make suitable definitions for φ_1 and φ_2.

First we will show that the formula for f works for southern latitudes and retrograde orbits. From the symmetry of the situation, it is clear that f should be the same for equal latitudes north and south. This justifies restricting L to nonnegative values in (1). Also from symmetry, f should be the same for i and $\pi - i$. If we regard f as a function of i, L, and λ, then we can show that this holds:

$$
\begin{aligned}
f(\pi - i, L, \lambda) &= \left[\varphi_1(\pi - i, L, \lambda) - \varphi_1(\pi - i, L, \lambda)\right]/\pi \\
&= \left[\arccos\left(\frac{-\sin\lambda + \sin L\cos(\pi - i)}{\cos L\sin(\pi - i)}\right) - \arccos\left(\frac{\sin\lambda + \sin L\cos(\pi - i)}{\cos L\sin(\pi - i)}\right)\right]\frac{1}{\pi} \\
&= \left[\arccos\left(\frac{-\sin\lambda - \sin L\cos i}{\cos L\sin i}\right) - \arccos\left(\frac{\sin\lambda - \sin L\cos i}{\cos L\sin i}\right)\right]\frac{1}{\pi} = f(i, L, \lambda)
\end{aligned}
$$

Thus, we need only consider cases with $0 \le i \le \pi/2$.

The remaining distinct geometries can be partitioned into five possible cases, which are identified as regions in Figure 6.

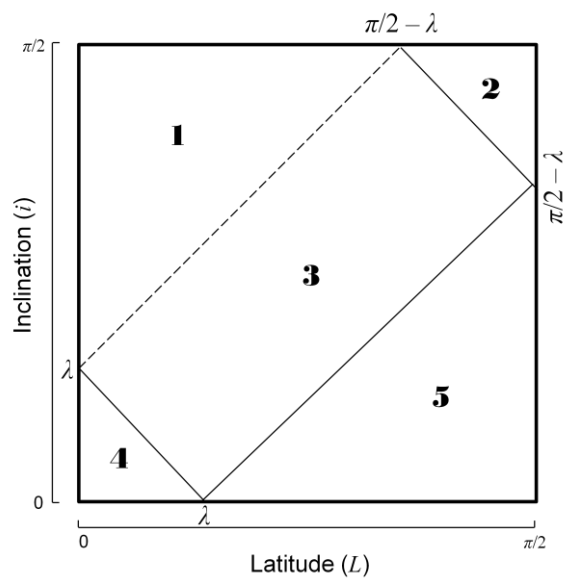

Figure 6. Five Cases for *f*

***Region 1*.** Latitude is low and inclination high enough for the spacecraft to miss north of the target. This is the situation in Figure 3 and Figure 4 for which we have derived equation (13) for φ_1 and (14) for φ_2.

***Region 2*.** Both latitude and inclination are high enough that there is a pass every rev. In this region we will retain the applicability of equation (12) by defining $\varphi_1 = \pi$ and $\varphi_2 = 0$. In this region also

$$i \geq -L + \pi - \lambda$$

$$i + L \geq \pi - \lambda \geq \pi / 2$$

$$\sin(i + L) \leq \sin(\pi - \lambda)$$

$$\sin i \cos L + \cos i \sin L \leq \sin \lambda$$

$$1 \leq \frac{\sin \lambda - \sin L \cos i}{\cos L \sin i}$$

$$-1 \geq \frac{-\sin \lambda + \sin L \cos i}{\cos L \sin i} \tag{15}$$

so we will get the correct value for cos φ_1 if we take the max of equation (13) and –1. Similarly,

$$i \leq L + \lambda$$

$$i - L \leq \lambda$$

$$\sin(i - L) \leq \sin(\lambda)$$

$$\sin i \cos L - \cos i \sin L \leq \sin \lambda$$

$$1 \leq \frac{\sin \lambda + \sin L \cos i}{\cos L \sin i} \tag{16}$$

and we will get the correct value for cos φ_2 if we take the min of equation (14) and 1.

Region 3. The spacecraft cannot miss north of the target but can miss south of it. In Figure 3 there would be no interval GH. The angle φ_1 can still be defined as in Figure 4, and equation (13) holds, but we will define $\varphi_2 = 0$ to preserve (12). In this region inequality (16) also holds, so cos φ_2 can again be found via a min of equation (14) and 1.

Region 4. Both latitude and inclination are low enough that there is a pass every rev. In this region we will again define $\varphi_1 = \pi$ and $\varphi_2 = 0$. Here

$$i < -L + \lambda$$

$$i + L \leq \lambda$$

$$\sin(i + L) \leq \sin(\lambda)$$

$$-1 \geq \frac{-\sin \lambda + \sin L \cos i}{\cos L \sin i} \tag{17}$$

so again we get the correct value for cos φ_1 with a max of equation (13) and –1. Inequality (16) still holds and cos φ_2 can be found with a min of equation (14) and 1.

Region 5. Latitude is high and inclination low enough that the spacecraft always passes south of the target and there is never a pass. Here we will define $\varphi_1 = \varphi_2 = 0$. Here

$$
\begin{aligned}
i &\le L - \lambda \\
L - i &\ge \lambda \\
\sin(L - i) &\ge \sin(\lambda) \\
\sin L \cos i - \cos L \sin i &\ge \sin \lambda \\
-1 &\ge \frac{\sin \lambda - \sin L \cos i}{\cos L \sin i} \\
1 &\le \frac{-\sin \lambda + \sin L \cos i}{\cos L \sin i}
\end{aligned}
\tag{18}
$$

and inequality (16) also applies, so cos φ_1 and cos φ_2 can be found with via mins with the expressions in (13) and (14) as in the other regions.

The only remaining case to consider is when the denominator in (13) and (14) is zero. This happens along the bottom and right edges of Figure 6, where $i = 0$ and/or $L = \pi/2$. Here we will define $\varphi_1 = \pi$ (region 2 or 4) or 0 (region 5) and $\varphi_2 = 0$.

The justification for equations (5) through (11) is now complete. The quantities F_1 and F_2 can be defined as the cosine of φ_1 and φ_2 respectively, where those angles are defined as above, based on the values of i and L and where they fall in Figure 6.

It is worth noting that there is a kind of duality between i and L in the numerator and denominators of (13) and (14), so that

$$
f(i, L, \lambda) = f\left(\frac{\pi}{2} - L, \frac{\pi}{2} - i, \lambda\right) \tag{19}
$$

2.3 Final Calculations

The formula for the orbital period P (10) is the standard one for Keplerian orbits (Bate, Mueller, and White, 1971, p. 33, eqn 1.7-9).

The length of a day divided by P gives the average number of revs. On a non-rotating Earth, the number of passes would be that quantity times f. However, on a rotating Earth an equatorial prograde orbit will have one fewer pass per day over a given (equatorial) target, an equatorial retrograde orbit one more, and a polar orbit the same number. The cos i term in (11) approximately accounts for this effect. With this, the derivation of the formula given in section 1.5 for PPD(i,h,ε,L) is complete.

Chapter 3: Accuracy of the Approximation

3.1 Cases Examined

The accuracy of the approximation was assessed by comparing its results to the results of simulations using STK in three sets of cases: a set of 20 cases sampling the five regions of Figure 6, including their retrograde and southern hemisphere equivalents; a complete 2^4 factorial analysis of the effect of changes in the four arguments around a typical base case; and a plot of PPD as a function latitude L for fixed i, h, and ε. In each case STK was run for three simulated years (1096 days) using the "J4Perturbation" propagator. Single runs were also done varying simulated duration, spacecraft right ascension of ascending node, spacecraft true anomaly at simulation start, and target longitude to verify that these parameters had no significant effect on the STK results (≤0.01 PPD). A similar run using the "HPOP" propagator, which is more accurate but runs much more slowly, verified that the choice of propagator also made no significant difference. In all the cases considered, the error of the approximation was less than 0.08 PPD and less than 1%, except in regions near $i = L \pm \lambda$, when the error could be as great as 0.22 PPD; by symmetry $\pi - i = L \pm \lambda$ will give similar errors.

3.2 Five Regions

Table 1 shows the results of calculating PPD using equations (3) through (11) compared to the results of using STK with the "J4Perturbation" propagator for five combinations of latitude L and inclination i located in approximately the centers of the five regions in Figure 6. All cases have a height h of 680 km and a minimum elevation ε of 30 degrees. Each region is tested for every combination of hemisphere and pro/retrograde, yielding 20 cases total. The greatest difference in absolute PPD is 0.07; the greatest difference in absolute percentage is 0.94%. The PPD results are also plotted in Figure 7, which shows the good agreement.

Table 1. Calculation and STK Results in Figure 6 Regions
(h=680 km, ε=30 deg)

	Label	i (deg)	N lat (deg)	PPD calculation	STK J4Pert for 1096 days Accesses	PPD	PPD Error	% error
North / Prograde	1NP	70	20	1.55	1698	1.55	0.00	0.08%
	2NP	87	87	14.59	16026	14.62	-0.03	-0.23%
	3NP	45	45	3.53	3902	3.56	-0.03	-0.94%
	4NP	3	3	13.64	14991	13.68	-0.04	-0.26%
	5NP	20	70	0.00	0	0.00	0.00	n/a
North / Retrograde	1NR	110	20	1.62	1782	1.63	0.00	-0.08%
	2NR	93	87	14.69	16026	14.62	0.07	0.49%
	3NR	135	45	3.88	4288	3.91	-0.03	-0.71%
	4NR	177	3	15.64	17189	15.68	-0.04	-0.28%
	5NR	160	70	0.00	0	0.00	0.00	n/a
South / Prograde	1SP	70	-20	1.55	1697	1.55	0.00	0.14%
	2SP	87	-87	14.59	16025	14.62	-0.03	-0.22%
	3SP	45	-45	3.53	3896	3.55	-0.03	-0.79%
	4SP	3	-3	13.64	14991	13.68	-0.04	-0.26%
	5SP	20	-70	0.00	0	0.00	0.00	n/a
South / Retrograde	1SR	110	-20	1.62	1780	1.62	0.00	0.04%
	2SR	93	-87	14.69	16025	14.62	0.07	0.49%
	3SR	135	-45	3.88	4288	3.91	-0.03	-0.71%
	4SR	177	-3	15.64	17189	15.68	-0.04	-0.28%
	5SR	160	-70	0.00	0	0.00	0.00	n/a

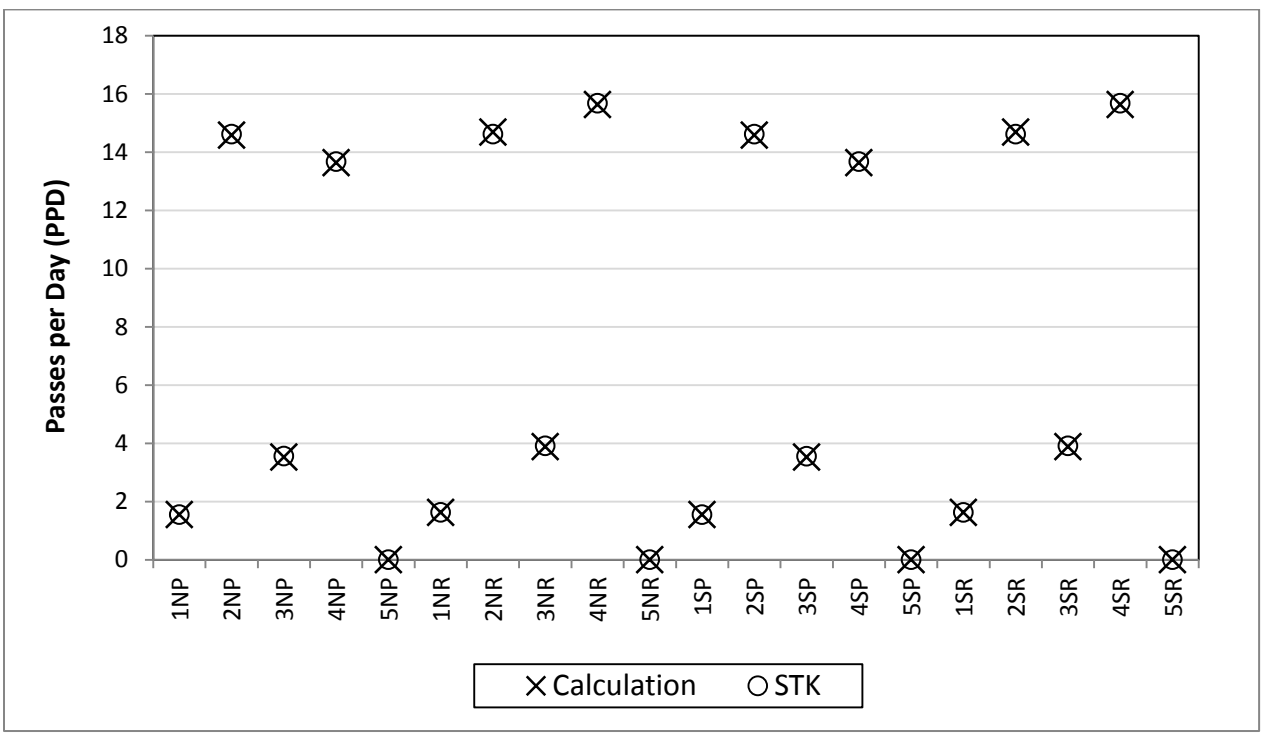

Figure 7. Plot of Table 1 Data

3.3 Factorial Analysis

To determine if error varied systematically with any combination of the arguments of the function PPD, it was checked for all sixteen possible combinations of high and low argument values around a typical middle case, all values being selected to stay in the region of nonzero PPD. The results are show in Table 2 and in Figure 8. The largest error occurred in the case labeled LLHH (i=50°, h=400 km, ε=45°, L=45°), where equations (3)-(11) yield 2.03 PPD and the STK simulation showed 2180 accesses in 1096 days, for 1.99 PPD, a difference of 0.04 PPD, or 1.94%. In this case, equation (4) yields λ=3.37°, so $L+\lambda$ is within 1.7° of i. This is the smallest difference between $L\pm\lambda$ and i in the table. It seems likely that what is happening is that there is a small range of longitudes of ascending node that result in the spacecraft missing north of the target even though the geometric approximation indicates a pass, resulting in a slight overestimate of PPD. More evidence for this hypothesis was found when exploring PPD as a function of latitude in Section 3.4. With the exception of the LLHH case, the largest absolute PPD error in Table 2 is 0.02 and the largest absolute percentage error is 0.55%. There is no significant pattern in the errors.

3.4 PPD as a Function of Latitude

To gain more insight into the behavior of the PPD function near $i=L\pm\lambda$, a series of cases were run varying L from zero to ninety degrees at one degree intervals in the critical areas, while keeping all other arguments constant, i at 75°, h at 400 km, and ε at 15°. The results are shown in Table 3 and in Figure 9. At L=65°, λ=9.98° and $L+\lambda$=74.98°≅i. Here the error is 0.22 PPD or 3.30%. At L=85°, λ=10.05° and $L-\lambda$=74.95°≅i. The error is 0.11 PPD; because the magnitude of PPD is very small the percentage error is high, 17.90%. These errors are the largest in the table by a great margin. Other than at these two latitudes, the largest absolute PPD error is 0.05 and the largest absolute percentage error is 0.98%. These data give additional confidence that the accuracy of the approximation formula in (3)-(11) is extremely good except near $i=L\pm\lambda$, and that even there the error in PPD is not great.

Table 2. 2^4 Factorial Analysis of Calculation vs. STK Results

Label	i (deg)	h (km)	ε (deg)	L (deg)	PPD Calculation	STK J4Pert for 1096 days Accesses	PPD	PPD Error	% Error
Baseline	60	680	30	35	2.10	2298	2.10	0.00	0.18%
HHHH	75	900	45	45	1.58	1722	1.57	0.01	0.49%
HHHL	75	900	45	15	1.10	1210	1.10	0.00	-0.25%
HHLH	75	900	15	45	4.15	4537	4.14	0.01	0.20%
HHLL	75	900	15	15	2.82	3098	2.83	0.00	-0.09%
HLHH	75	400	45	45	0.87	951	0.87	0.00	0.55%
HLHL	75	400	45	15	0.60	664	0.61	0.00	-0.49%
HLLH	75	400	15	45	2.57	2808	2.56	0.01	0.27%
HLLL	75	400	15	15	1.77	1936	1.77	0.00	0.09%
LHHH	50	900	45	45	3.82	4206	3.84	-0.01	-0.34%
LHHL	50	900	45	15	1.39	1521	1.39	0.00	-0.20%
LHLH	50	900	15	45	5.42	5963	5.44	-0.02	-0.33%
LHLL	50	900	15	15	3.61	3956	3.61	0.00	-0.06%
LLHH	50	400	45	45	2.03	2180	1.99	0.04	1.94%
LLHL	50	400	45	15	0.76	828	0.76	0.00	0.47%
LLLH	50	400	15	45	4.84	5320	4.85	-0.01	-0.23%
LLLL	50	400	15	15	2.24	2458	2.24	-0.01	-0.29%

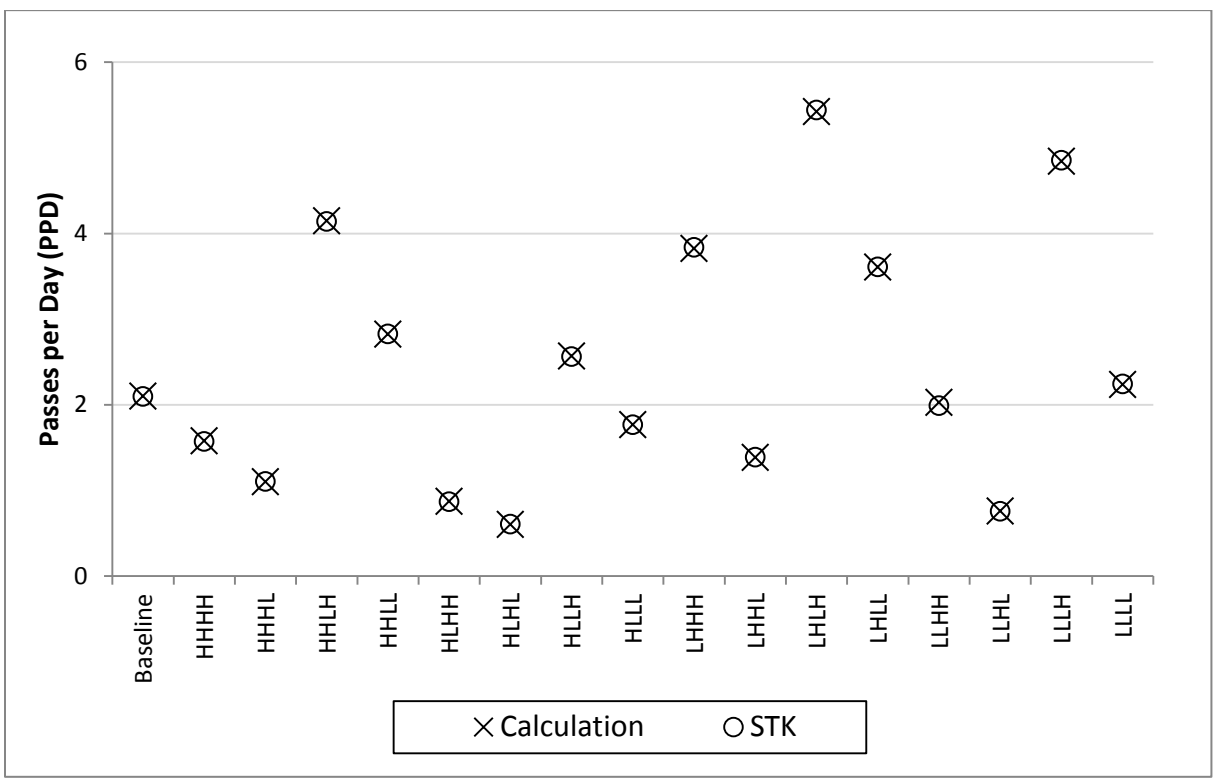

Figure 8. Plot of Table 2 Data

Table 3. PPD as a Function of Latitude
(i=75 deg, h=400 km, ε=15 deg)

L (deg)	PPD Calc.	STK J4Pert for 1096 days Accesses	PPD	PPD Error	% Error	L (deg)	PPD Calc.	STK J4Pert for 1096 days Accesses	PPD	PPD Error	% Error
0	1.70	1862	1.70	0.00	-0.08%	64	5.56	6033	5.50	0.05	0.98%
5	1.71	1870	1.71	0.00	-0.06%	65	6.74	7150	6.52	0.22	3.30%
10	1.73	1894	1.73	0.00	0.01%	66	6.87	7500	6.84	0.02	0.33%
15	1.77	1936	1.77	0.00	0.09%	67	6.81	7442	6.79	0.02	0.30%
20	1.83	2003	1.83	0.00	-0.09%	68	6.75	7385	6.74	0.01	0.20%
25	1.91	2085	1.90	0.00	0.16%	69	6.69	7322	6.68	0.01	0.11%
30	2.01	2201	2.01	0.00	0.11%	70	6.62	7251	6.62	0.00	0.04%
35	2.15	2352	2.15	0.00	0.09%	75	6.15	6760	6.17	-0.02	-0.31%
40	2.33	2547	2.32	0.00	0.19%	80	5.21	5752	5.25	-0.03	-0.66%
45	2.57	2808	2.56	0.01	0.27%	81	4.89	5394	4.92	-0.03	-0.67%
50	2.90	3169	2.89	0.01	0.30%	82	4.46	4929	4.50	-0.03	-0.73%
55	3.38	3692	3.37	0.02	0.45%	83	3.88	4282	3.91	-0.03	-0.77%
60	4.18	4554	4.16	0.03	0.63%	84	2.96	3272	2.99	-0.02	-0.69%
61	4.42	4811	4.39	0.03	0.62%	85	0.73	681	0.62	0.11	17.90%
62	4.70	5118	4.67	0.03	0.66%	86	0.00	0	0.00	0.00	n/a
63	5.06	5499	5.02	0.04	0.82%	90	0.00	0	0.00	0.00	n/a

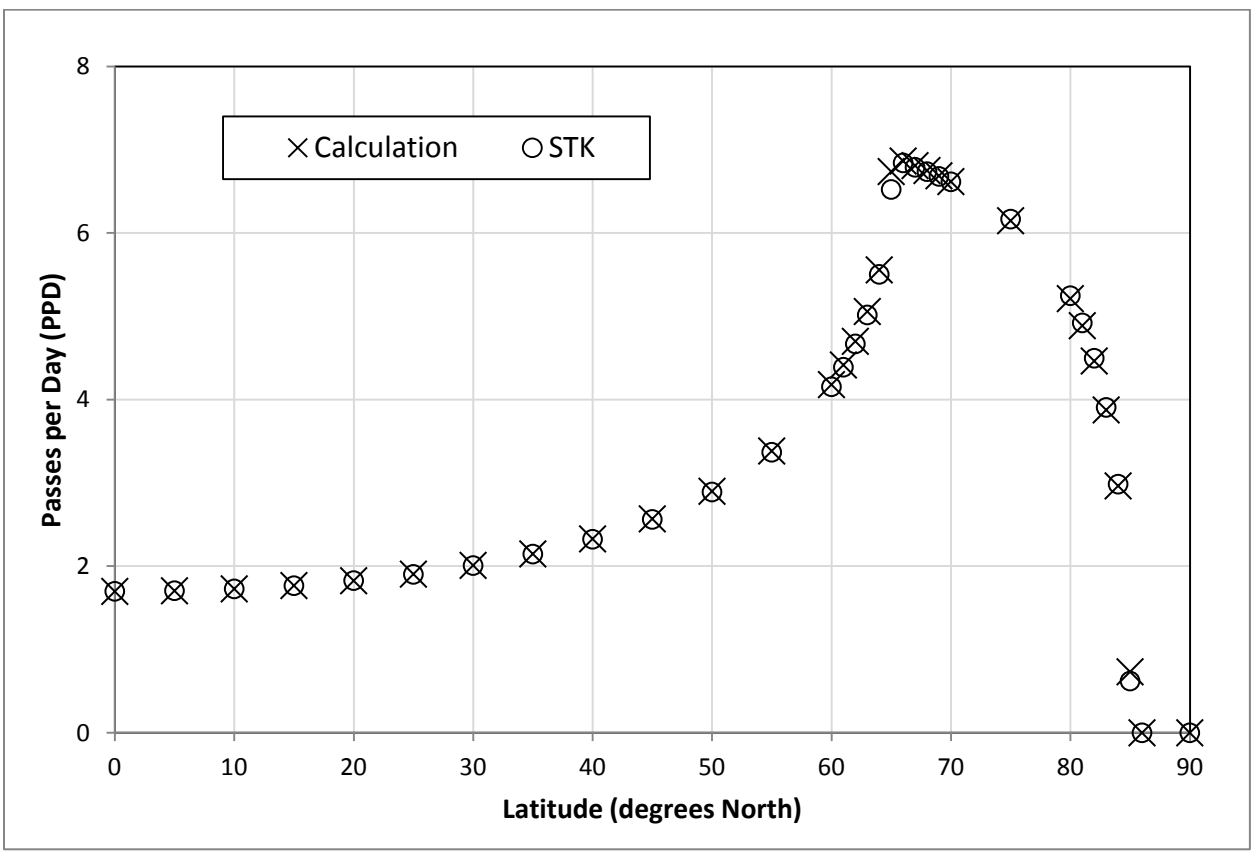

Figure 9. Plot of Table 3 Data

Chapter 4: Excursions around a Base Case

4.1 The Base Case

With an accurate closed-form expression for passes per day, it becomes easy and convenient to explore how this figure of merit changes for different orbits and target locations. This chapter gives some examples of how this flexibility can be exploited to increase understanding of the behavior of this metric as the variables change. PPD is a function of four variables: i, h, ε, and L. In the following sections are charts showing how PPD varies as one, two, or three of its arguments change between wide limits, while holding the remaining argument(s) at fixed base values. These base values are shown in Table 4. They were chosen to be realistic but not near the limits of variation. With these values, PPD ≅ 2.1006.

Table 4. A Base Case

Parameter	Base Value	Remarks	Variation	Remarks
Inclination (i)	60°	Good temperate-zone coverage	0-90°	Retrograde orbits are similar
Altitude (h)	680 km	Similar to altitudes of Ikonos and GeoEye commercial imagery spacecraft	350-1000 km	Covers almost all LEO satellites in NORAD catalog
Minimum Elevation (ε)	30°	Allows reasonable imaging	0-90°	
Latitude (L)	35°	Malta, Kirkuk, Tehran, Tokyo, Albuquerque, Memphis (TN); Buenos Aires, Sydney	0-90°	North and south latitudes give identical results

4.2 Varying One Parameter

Figure 10 through Figure 13 show PPD as a function of i, h, ε, and L, respectively, holding all other values at their base levels from Table 4. A dot indicates the base case itself. Figure 10 looks like a mirror image of Figure 13 because of the duality between i and L in equation (19). Charts like these are not unusual; Figure 13 for instance corresponds exactly to Figure 9-45 in Wertz (2001). The approximation formula makes them easier.

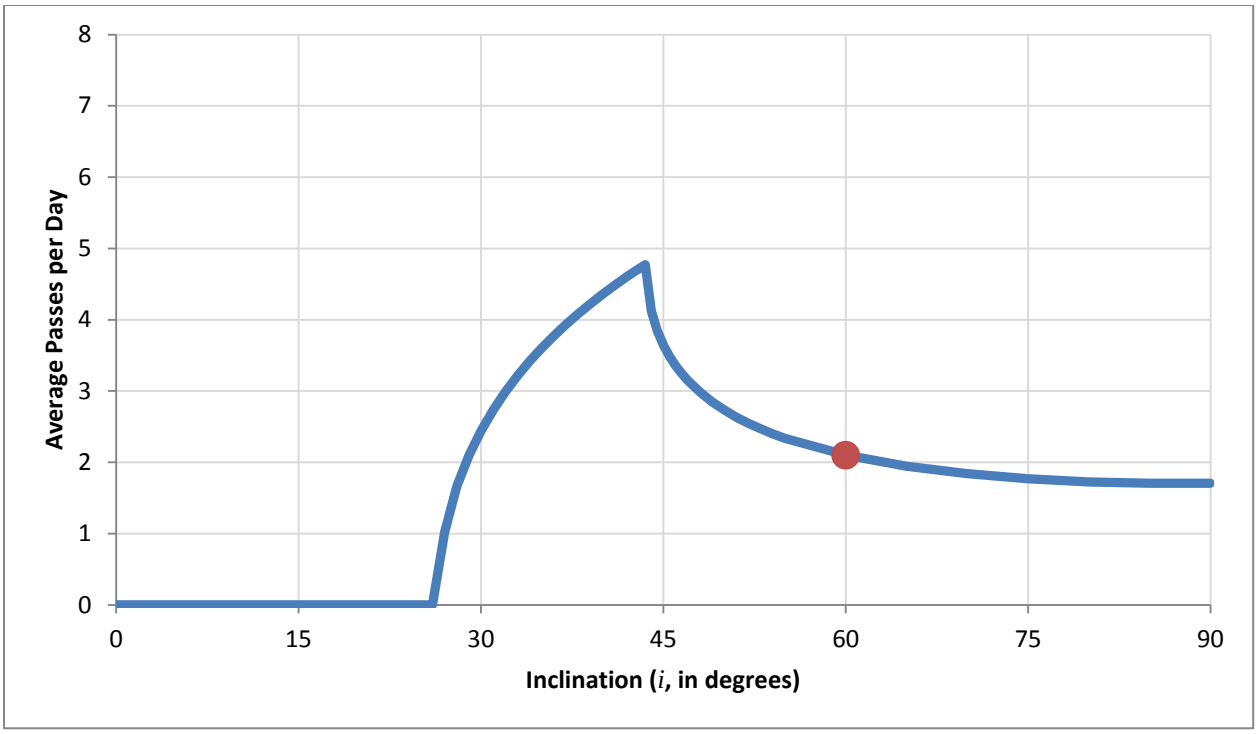

Figure 10. PPD as a Function of *i* for the Base Case

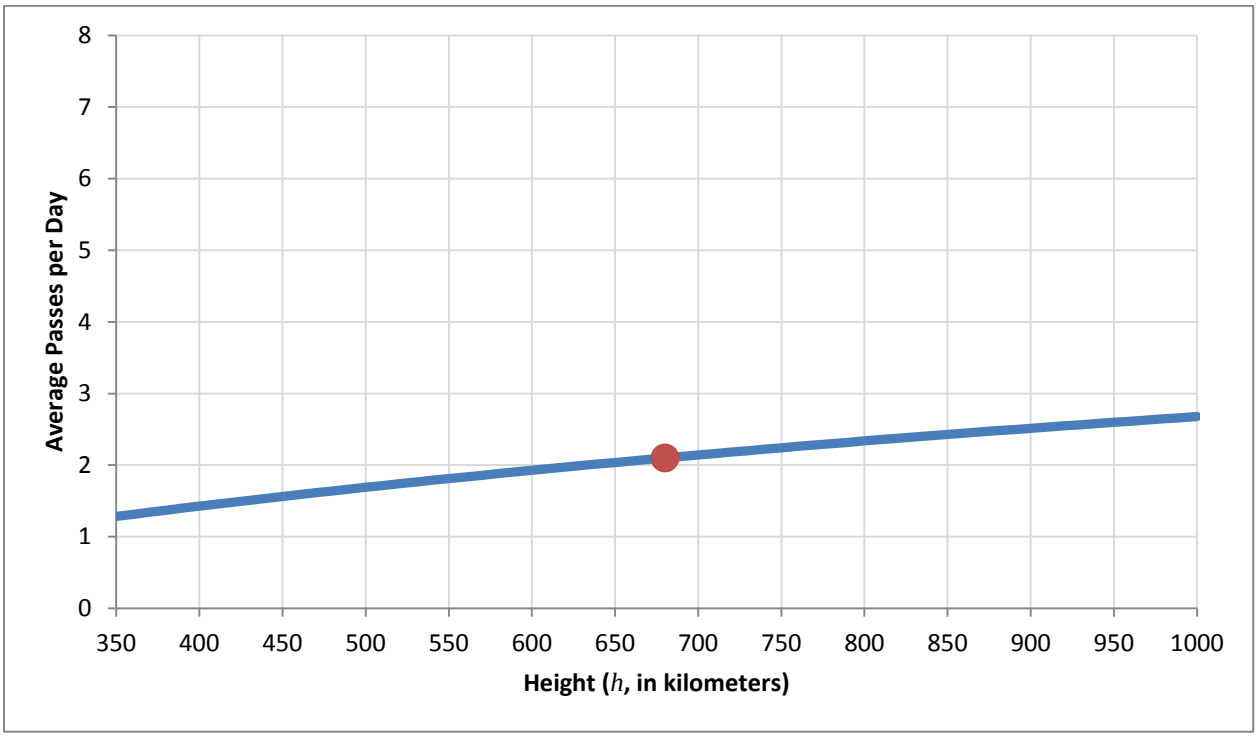

Figure 11. PPD as a Function of *h* for the Base Case

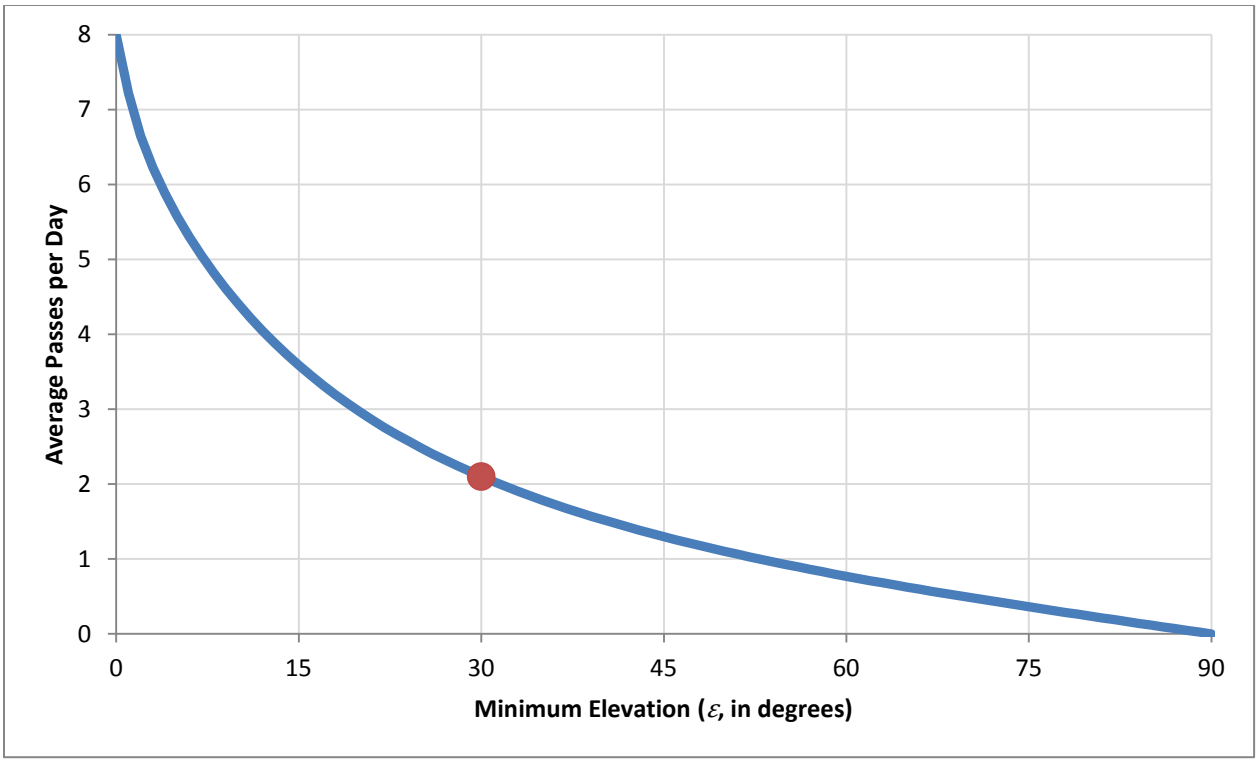

Figure 12. PPD as a Function of ε for the Base Case

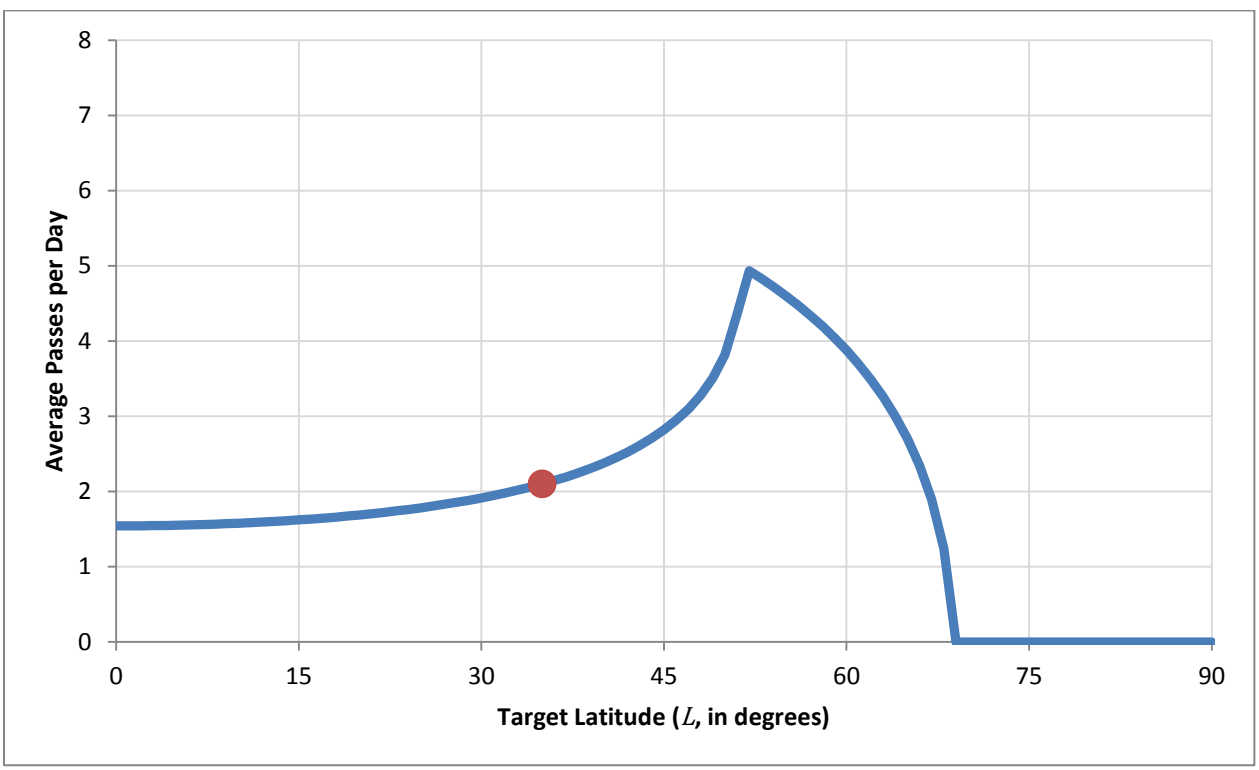

Figure 13. PPD as a Function of *L* for the Base Case

4.3 Varying Two Parameters

New insights can come when one plots PPD as a function of two of its four arguments. This section provides contour plots for all six possible combinations. Figure 14 shows PPD as a function of inclination (i) and latitude (L), with altitude (h) and elevation (ε) fixed at their base values from Table 4. The axis lines are placed at these base values, and the intersection is at the base case itself. This chart has the same axes as Figure 6 on p. 21, and the correlation of PPD with the regions in that figure is evident. (With these values of h and ε, $\lambda \cong 8.6°$.) In regions 2 and 4, both target and orbit are polar or equatorial, respectively, and PPD is at its maximum of one per rev (before adjusting for latitude). In region 5, the target is too far north or south for the spacecraft ever to see it, so PPD is identically zero. In region 3, the spacecraft sees the target on certain revs, but never crosses the target's longitude out of sight of it towards the pole, and PPD can be 4.4 or higher at any latitude. In region 1, the spacecraft can pass the target's longitude out of sight both north and south of it. PPD decreases as the orbit becomes polar and the target equatorial, reaching a minimum of about 1.4 when i = 90° and L = 0°.

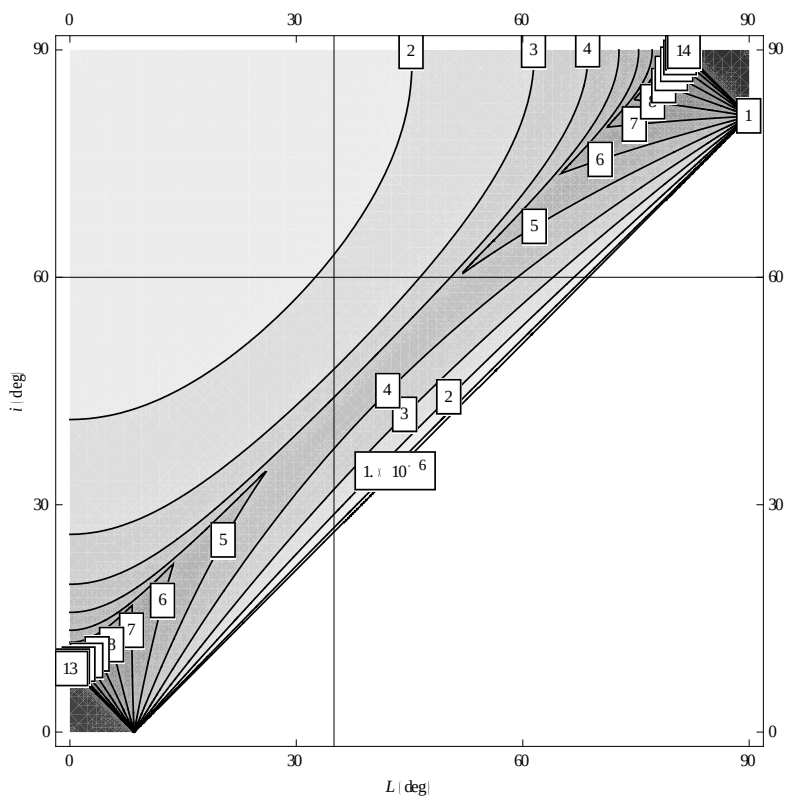

Figure 14. PPD as a Function of *i* and *L*, with *h* = 680 km and ε = 30°

Figure 15 shows PPD as a function of ε and L. The primary effect of increasing ε is to reduce λ, i.e. reduce the size of the circle the spacecraft must cross to see the target. On the right side of this figure, the target is too far north for the spacecraft to see with i = 60°, so PPD is identically zero. On the left side, PPD decreases as ε increases and the target approaches the Equator, becoming zero at the top of the chart, where $\varepsilon = 90°$ and the spacecraft is required to pass directly over the target to see it.

Figure 16 shows PPD as a function of ε and i. It looks like a mirror image of Figure 15 because of the duality between i and L in equation (19). On the left, inclination is so low that the spacecraft never sees the target. On the right, PPD decreases to zero as ε increases to 90°.

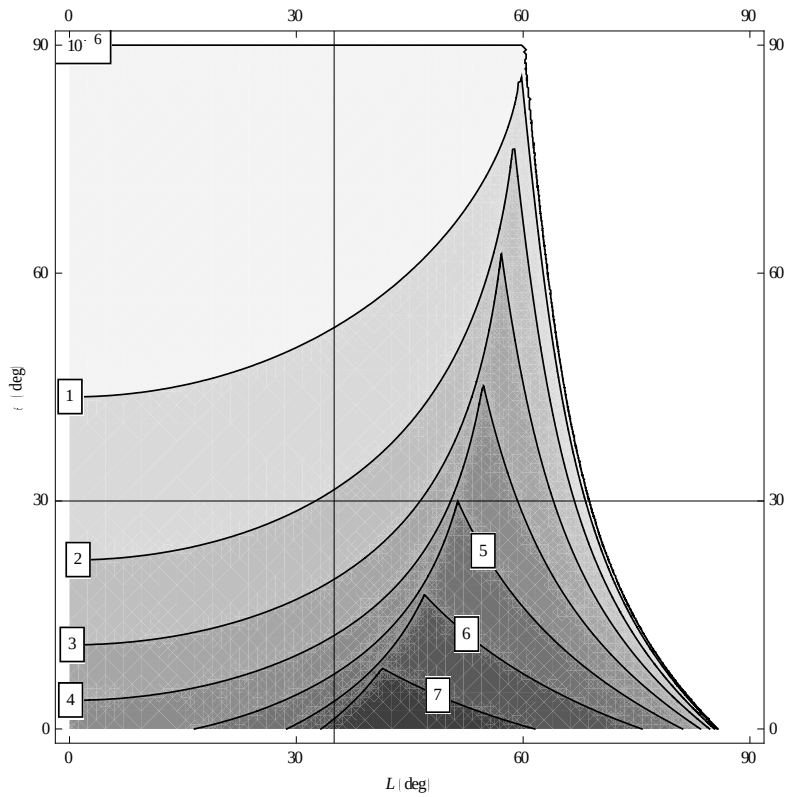

Figure 15. PPD as a Function of ε and L, with h = 680 km and i = 60°

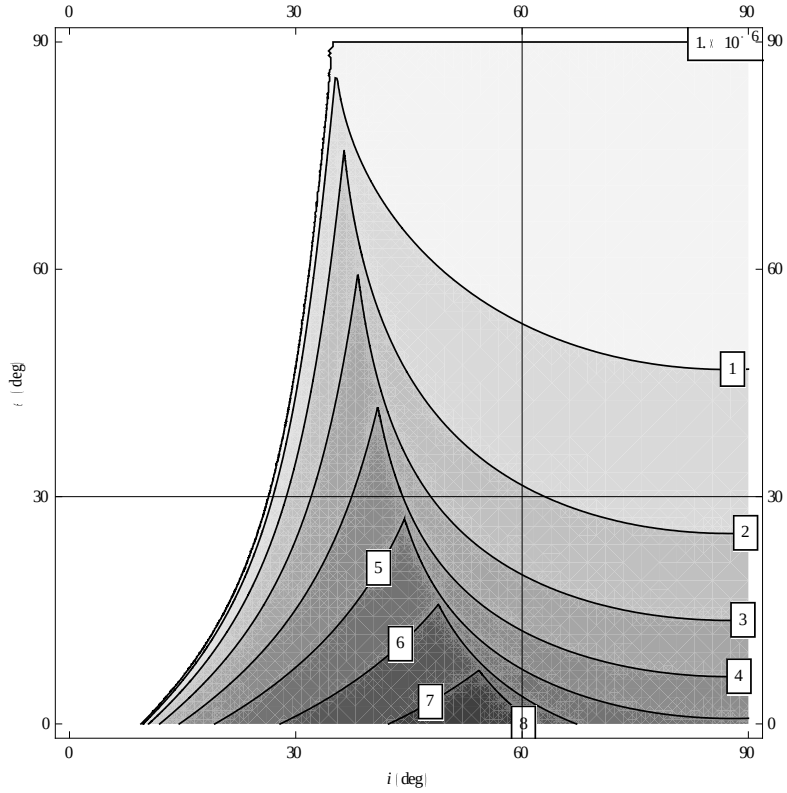

Figure 16. *PPD* as a Function of ε and i, with h = 680 km and L = 35°

Figure 17 and Figure 18 show PPD as a function of h and i and of h and L, respectively. Again the duality between i and L is evident. However, the figures are not perfect mirror images. The parameters i and L have symmetric effects on f in equation (9), but they have differing if relatively minor effects in equations (3) and (11), and thus slightly nonsymmetrical effects on PPD. In both figures, PPD increases as h increases, because that also increases λ (though increasing h also increases the period and therefore reduces the number of revs per day, a partially countervailing effect). Along the horizontal axis, on one side the target is always out of sight to poleward of the spacecraft, and on the other the spacecraft can pass both north and south of the target.

The final chart is Figure 19, which shows the effect on PPD of h and ε. These two parameters control the size of λ, though it is evident in the chart that the major effect is from ε.

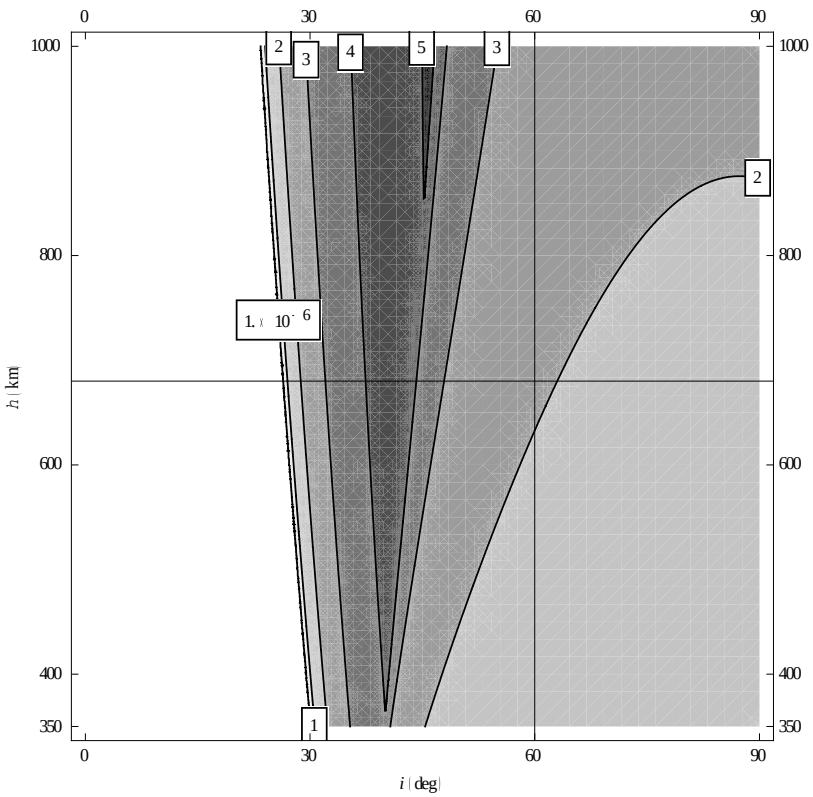

Figure 17. *PPD* as a Function of *h* and *i*, with *ε* = 30° and *L* = 35°

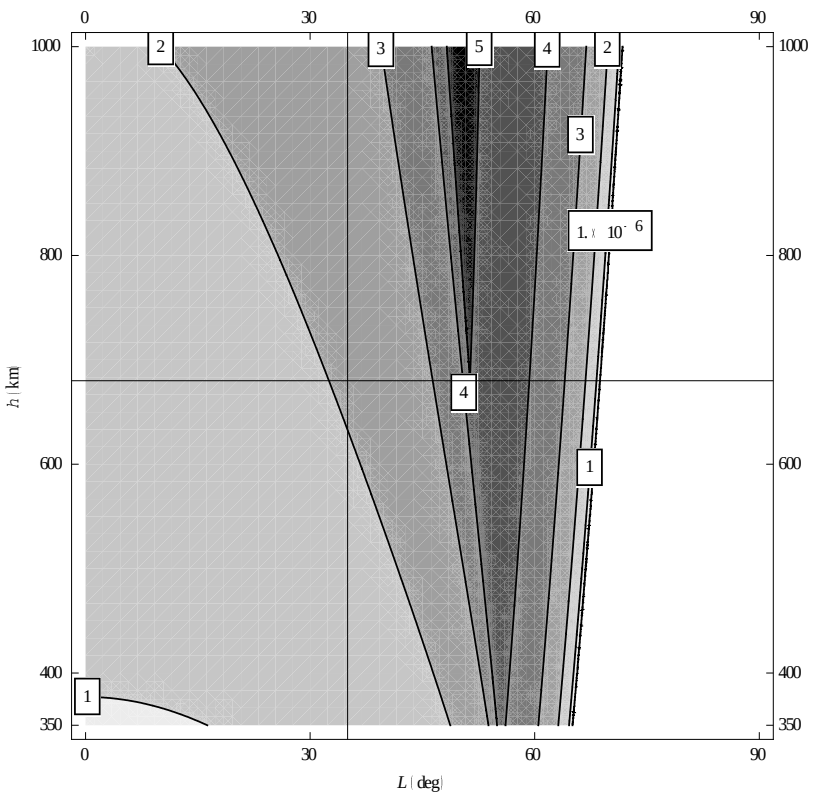

Figure 18. *PPD* as a Function of *h* and *L*, with *ε* = 30° and *i* = 60°

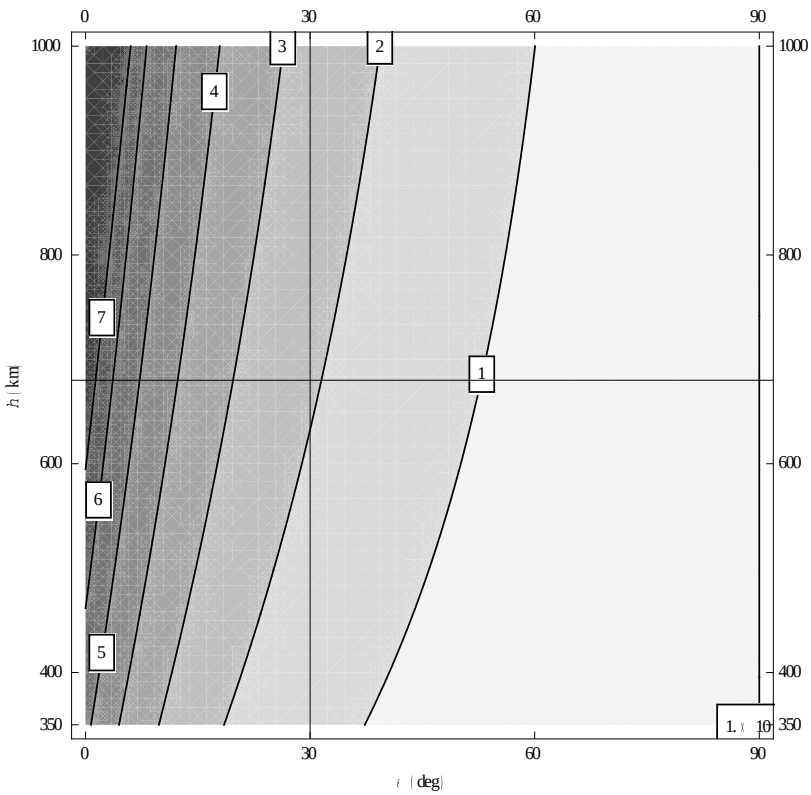

Figure 19. *PPD* as a Function of *h* and *ε*, with *L* = 35° and *i* = 60°

4.4 Varying Three Parameters

Figure 20 shows the surface where PPD is equal to its base case value of 2.10, holding *h* at 680 km because it is the least important parameter. Lower values of PPD are above the surface and higher values below. The base case itself is on the surface at the intersection of the dashed line for $\varepsilon = 30°$ and the dot-dashed line for $i = 60°$.

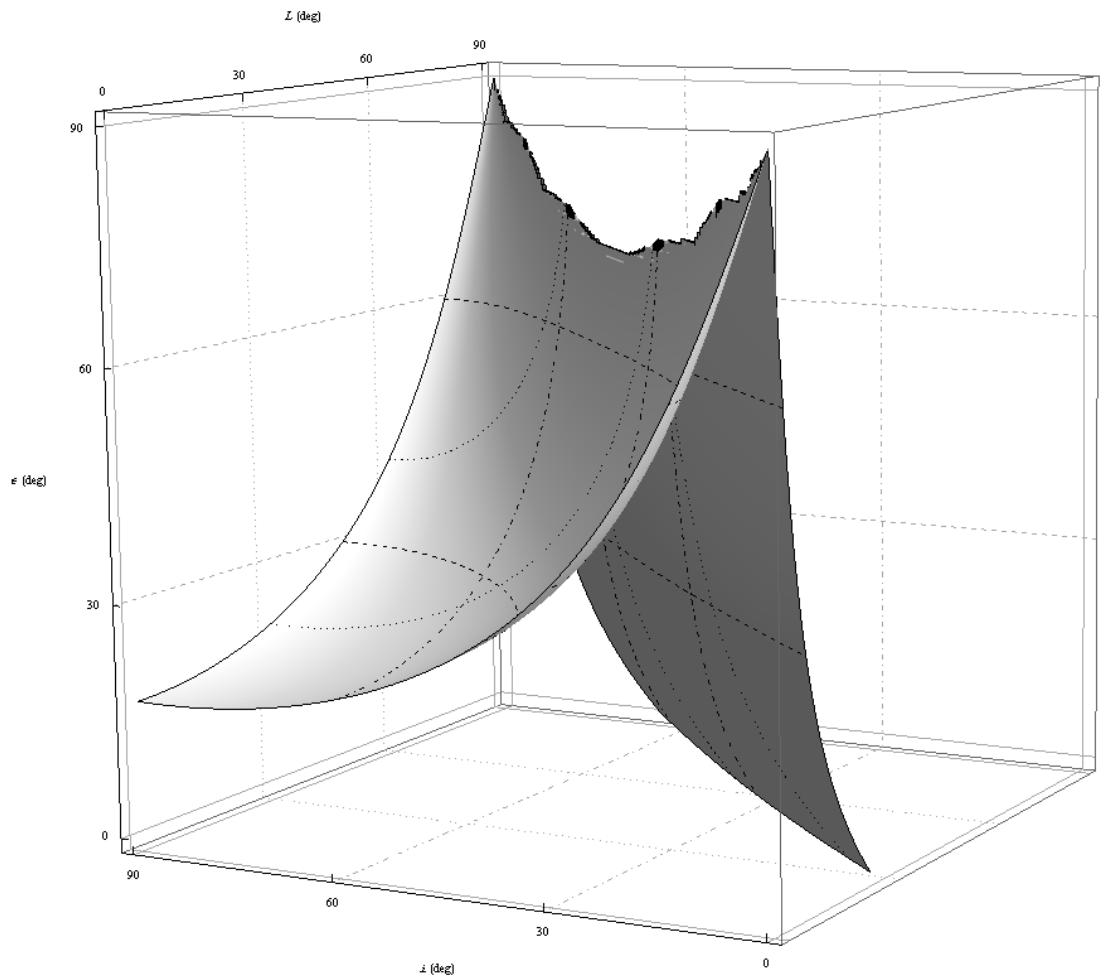

Figure 20. *PPD* = 2.10 Surface (*h* = 680 km)

Chapter 5: Sensitivity to Assumption of Circularity

The geometrical development in Chapter 2: is based on the assumption that the orbit is circular. The effect of eccentricity on PPD when holding all other parameters constant was explored using the base case in Table 4. STK simulations were run for that case modified with eccentricities from 0.00 to 0.07. PPD decreased slowly as eccentricity increased, being 5.3% below the e = 0.00 result when e = 0.07. The results are shown in Table 5 and Figure 21.

Table 5. Variation of PPD with Eccentricity for Base Case

Eccentricity	Orbit Height (km)	Average PPD	Difference from e = 0 case
Assumed 0 (calculation)	680	2.101	0.20%
0	680 x 680	2.096	N/A
0.01	609 x 751	2.092	-0.19%
0.02	539 x 821	2.092	-0.23%
0.03	468 x 892	2.075	-1.01%
0.04	398 x 962	2.063	-1.60%
0.05	327 x 1033	2.036	-2.88%
0.06	257 x 1103	2.011	-4.09%
0.07	186 x 1174	1.985	-5.30%

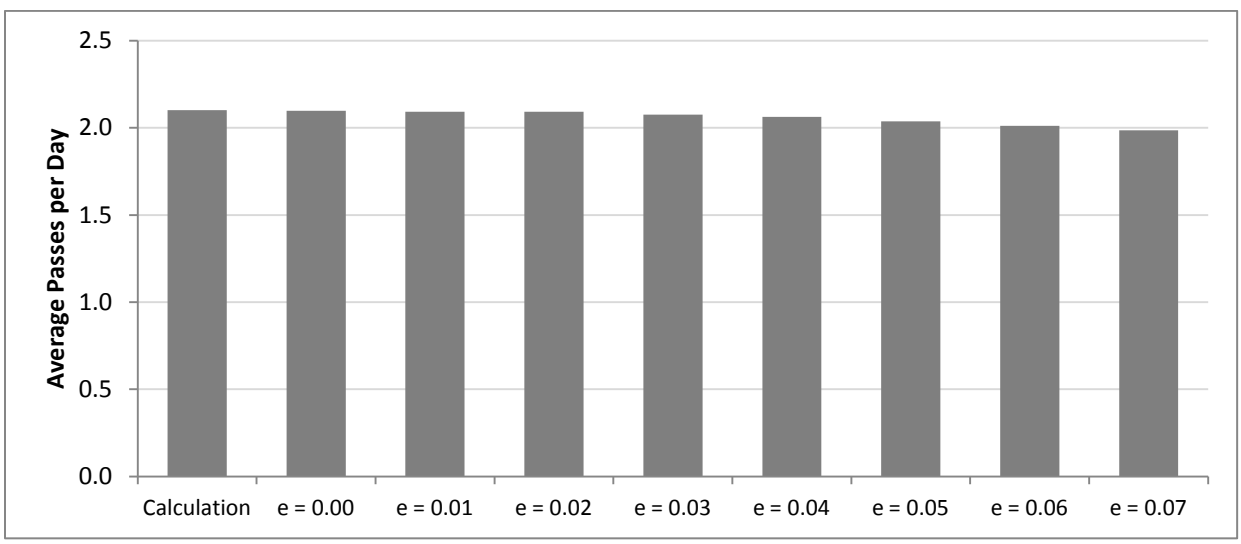

Figure 21. Variation of PPD with Eccentricity for Base Case

More significant that the slight decrease in long-term average PPD with increasing eccentricity is the short-term change in PPD as the line of apsides rotates. When the apogee of the orbit is near the latitude of the target, the added height results in a greater swath of visibility, so more of the revs include a pass. When it is perigee that is at the target's latitude, the swath is narrow and fewer revs include a pass. The line of apsides for the base case moves about 0.88 degrees per day, caused predominately by the oblateness of the Earth, according to equations 6-16 through 6-20 in Boden (1999), so a given latitude alternates between seeing apogee and perigee every 204 days. The simulations with different eccentricities were run over 1224 simulated days (three complete rotation of the line of apsides) and averages taken every complete calendar month. The results for sixteen months that together span a complete rotation are shown in Figure 22. For the e=0.07 case, the monthly averages were as much as 38% above and 46% below the long run average for the circular case.

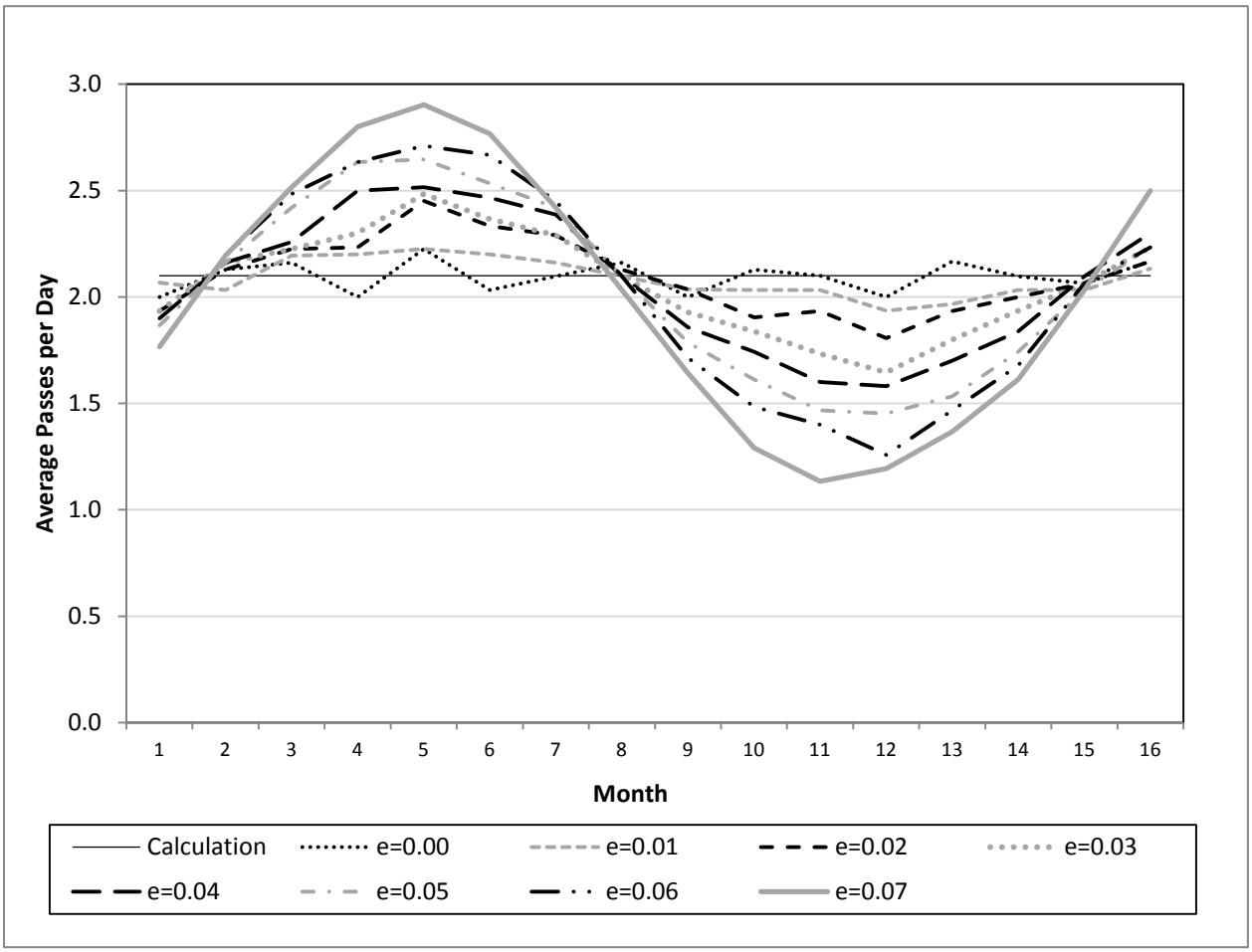

Figure 22. Month-to-Month Variation of PPD with Eccentricity for Base Case

The e=0.00 line in Figure 22 also gives some insight into how short-term PPD varies from the long-term average for a circular orbit. The 1224 simulated days included 39 complete months. The monthly averages varied from 2.00 (-4.8%) to 2.23 (+6.0%), compared to the 1224-day average of 2.10, with a standard deviation of 0.07 passes per day (3.2%). Of course, the monthly averages are not independent: the lag-1 autocorrelation for this sample was -0.64.

Chapter 6: Conclusion

This report has shown that an accurate approximation of the long-run average number of passes per day for a given target latitude and a given circular low Earth orbit can be calculated in closed form. This approximation can simplify the orbit selection and optimization process when PPD is an important criterion. The calculation also enables a new way to think about PPD. It is usually thought of as a performance metric that is to be calculated for each of a set of discrete cases. In this report, it is thought of as a continuous function of four variables. This flexible and unified way of looking at it provides new insights into how passes per day changes for different targets and different orbit configurations. It can be used as the objective function of an optimization routine in mathematical programming. It helps increase our understanding of how low-orbit spacecraft can interact with terrestrial targets.

Bibliography

Bate, R. R., Mueller, D. D., and White, E. W. 1971. *Fundamentals of Astrodynamics*. New York: Dover.

Boden, G. B. 1999. Chapter 6: Introduction to Astrodynamics. In J. R. Wertz and W. J. Larson (Eds.), *Space Mission Analysis and Design*. El Segundo, CA: Microcosm.

Lang, T. J. 1984. Orbital Constellations which Minimize Revisit Time. In *Proceedings of the AAS/AIAA Conference, Lake Placid, NY, August 1983*. San Diego, CA: Univelt.

Santos, M., and Shapiro, B. 2007. Improving the Coverage of Earth Targets by Maneuvering Satellite Constellations (Report AFRL-SR-AR-TR-07-0393). Arlington, VA: Air Force Office of Scientific Research.

Santos, M., and Shapiro, B. 2008. Relating Satellite Coverage to Orbital Geometry (Paper AIAA 2008-6609). Reston, VA: American Institute of Aeronautics and Astronautics.

Wertz, J. R. 1999. Chapter 7: Orbit and Constellation Design. In J. R. Wertz and W. J. Larson (Eds.), *Space Mission Analysis and Design*. El Segundo, CA: Microcosm.

Wertz, J. R. 2001. *Mission Geometry; Orbit and Constellation Design and Management*. El Segundo, CA: Microcosm.

Appendix A: List of Abbreviations*

L	
LEO	Low Earth Orbit
N	
NORAD	North American Aerospace Defense Command
P	
PPD	passes per day
S	
STK	software for system modeling and mission analysis in space and related applications sold by Analytical Graphics, Inc. (no expansion)
U	
USMA	United States Military Academy

*This table is sorted alphabetically

Distribution List

NAME/AGENCY	ADDRESS	COPIES
Roger Chapman Burk	Department of Systems Engineering Mahan Hall West Point, NY 10996	5
Dr. Steve F. Pierce Director	Decision Support Directorate Future Warfare Center USA Space & Missile Defense Command Redstone Arsenal, AL 35898	1
Paul Alexander Page Chief	Studies and Analysis Division Decision Support Directorate Future Warfare Center USA Space & Missile Defense Command Redstone Arsenal, AL 35898	1
David L. Silvernail Tactical Analysis Team Lead	Studies & Analysis Division Decision Support Directorate Future Warfare Center USA Space & Missile Defense Command Redstone Arsenal, AL 35898	1
Dean, USMA	Office of the Dean Building 600 West Point, NY 10996	1
Defense Technical Information Center (DTIC)	ATTN: DTIC-O Defense Technical Information Center 8725 John J. Kingman Rd, Suite 0944 Fort Belvoir, VA 22060-6218	1
Department Head-DSE	Department of Systems Engineering Mahan Hall West Point, NY 10996	1
ORCEN	Department of Systems Engineering Mahan Hall West Point, NY 10996	5

NAME/AGENCY	ADDRESS	COPIES
ORCEN Director	Department of Systems Engineering Mahan Hall West Point, NY 10996	1
USMA Library	USMA Library Bldg 757 West Point, NY 10996	1

REPORT DOCUMENTATION PAGE – SF298

Form Approved
OMB No. 0704-0188

Public reporting burden for this collection of information is estimated to average 1 hour per response, including the time for reviewing instructions, searching existing data sources, gathering and maintaining the data needed, and completing and reviewing this collection of information. Send comments regarding this burden estimate or any other aspect of this collection of information, including suggestions for reducing this burden to Department of Defense, Washington Headquarters Services, Directorate for Information Operations and Reports (0704-0188), 1215 Jefferson Davis Highway, Suite 1204, Arlington, VA 22202-4302. Respondents should be aware that notwithstanding any other provision of law, no person shall be subject to any penalty for failing to comply with a collection of information if it does not display a currently valid OMB control number. **PLEASE DO NOT RETURN YOUR FORM TO THE ABOVE ADDRESS.**

1. REPORT DATE *(DD-MM-YYYY)*
23-09-2011

2. REPORT TYPE
Technical Report

3. DATES COVERED *(From - To)*

4. TITLE AND SUBTITLE

A Closed-Form Approximation of Revisit Rate for Low-Altitude Spacecraft

5a. CONTRACT NUMBER

5b. GRANT NUMBER

5c. PROGRAM ELEMENT NUMBER

6. AUTHOR(S)

Roger Chapman Burk

5d. PROJECT NUMBER

5e. TASK NUMBER

5f. WORK UNIT NUMBER

7. PERFORMING ORGANIZATION NAME(S) AND ADDRESS(ES)

Dept of Systems Engineering
US Military Academy
West Point, NY 10996

8. PERFORMING ORGANIZATION REPORT NUMBER

9. SPONSORING / MONITORING AGENCY NAME(S) AND ADDRESS(ES)

10. SPONSOR/MONITOR'S ACRONYM(S)

11. SPONSOR/MONITOR'S REPORT NUMBER(S)

12. DISTRIBUTION / AVAILABILITY STATEMENT
Distribution A – Approved for Public Release – Distribution Unlimited

13. SUPPLEMENTARY NOTES

14. ABSTRACT

This report develops a closed-form, continuous, and piecewise differentiable function that gives average revisits per day as a function of orbit altitude, orbit inclination, target latitude, and minimum required elevation. The function is compared to the results of astrodynamic simulations and shown to accurate to within 0.08 passes per day and 1% in almost all cases. It allows instant calculation of an excellent approximation of this important performance parameter, and could be used as part of an optimization routine. The convenience and flexibility provided by this function are demonstrated in a series of charts showing passes per day as a function of one, two, and three variables. The function assumes a circular orbit; the sensitivity of the result to eccentricity is explored using astrodynamic simulations, and is found to decrease by 5.3% as eccentricity increases to 0.07 for a typical case.

15. SUBJECT TERMS
Satellites, Orbits, Astrodynamics

16. SECURITY CLASSIFICATION OF:			**17. LIMITATION OF ABSTRACT**	**18. NUMBER OF PAGES**	**19a. NAME OF RESPONSIBLE PERSON**
					Roger Chapman Burk
a. REPORT	**b. ABSTRACT**	**c. THIS PAGE**		ix + 48	**19b. TELEPHONE NUMBER** *(include area code)*
Unclassified	Unclassified	Unclassified			845-938-4754

Standard Form 298 (Rev. 8-98)
Prescribed by ANSI Std. Z39.18